Spin-filter effect of ferromagnetic europium sulfide tunnel barriers

X. Hao, J. S. Moodera, and R. Meservey
Francis Bitter National Magnet Laboratory, Massachusetts Institute of Technology, Cambridge, Massachusetts 02139
(Received 23 March 1990)

We have observed electron-spin polarization in the tunnel current in metal-EuS-metal junctions. The value of polarization can be as high as 85%. This polarization is attributed to the exchange splitting of the EuS conduction band as a result of the ferromagnetic transition occurring in EuS at about 15 K. This conduction-band splitting lowers the tunnel barrier height for spin-up electrons and raises it for spin-down electrons, giving rise to spin polarization in the tunnel current. Tunnel barrier lowering is also manifested in the observed decrease of junction resistance with temperature below 15 K. The exchange interaction between quasiparticles in Al and the magnetic Eu^{2+} ions in EuS greatly enhances the Zeeman splitting of the superconducting quasiparticle density of states; in fact, some junctions show Zeeman splitting corresponding to an internal field of $B_i^* = 3$ T before any external magnetic field is applied.

INTRODUCTION

Spin-polarized tunneling was developed based on the Zeeman splitting of the quasiparticle density of states (DOS) of a superconductor. This Zeeman splitting was first observed in thin-film Al superconductors,[1] and then in some other superconducting elements and alloys: V and V-Ti alloy,[2,3] amorphous Ga,[4,5] and V_3Ga.[6] As an experimental technique, it has been used to measure the spin polarization of the itinerant electrons in $3d$ metals and alloys and in $4f$ metals.[7–9] When tunneling from a ferromagnetic electrode into a superconductor whose DOS is split by a magnetic field, the majority electrons contribute more than the minority electrons to the total tunnel conductance for each of the ferromagnets measured to date, resulting in an asymmetric tunnel conductance curve with respect to bias voltage. From the asymmetry one can calculate the degree of spin polarization of the itinerant electrons at the Fermi level. So far aluminum has been most successful as the spin-selective electrode in spin-polarized tunneling experiments partly because of the relative ease in fabricating aluminum junctions, and partly because of its small spin-orbit scattering.[10] Vanadium has also been successfully used as a spin-selective electrode in superconductor-ferromagnet tunneling, despite the many difficulties in junction fabrication.[3]

In previous spin-polarized tunneling studies, polarization of the tunnel current comes from the different densities of spin-up, spin-down conduction electrons at the Fermi level in the ferromagnetic electrode.[11] In the present study, instead of having magnetic electrodes, we used a ferromagnetic semiconductor (EuS) as the tunnel barrier. Spin polarization in the tunnel current arises from different barrier heights for electrons with different spin orientations when the conduction band of EuS splits into spin-up and spin-down subbands. Bulk EuS has a band gap of 1.65 eV and a Curie temperature of $T_m = 16.6$ K.[12] The exchange splitting of the EuS conduction band in the ferromagnetic state was discovered and studied by measuring the red shift of the optical-absorption edge. This splitting essentially reaches its full value of $\Delta E_{ex} = 0.36$ eV by 4 K.[13] When EuS is used as a tunnel barrier, the barrier height for spin-up (-down) electrons is changed by the conduction-band splitting: $\phi_{\uparrow,\downarrow} = \phi_0 \mp \Delta E_{ex}(T)/2$, where ϕ_0 is the average barrier height above T_m. Since the tunneling process depends sensitively on the barrier height, the splitting of the EuS conduction band greatly increases the probability of tunneling for spin-up electrons and reduces that for spin-down electrons (see Fig. 1). This is called the spin-filter effect. It has been observed directly in field-emission experiments where electrons emitted from EuS-coated tungsten tips were found to have a high degree of spin polarization, $P = 89 \pm 7\%$.[14,15] Early tunneling experiments using Eu chalcogenides as barriers also demonstrated indirectly the spin-filter effect by observing the decrease of

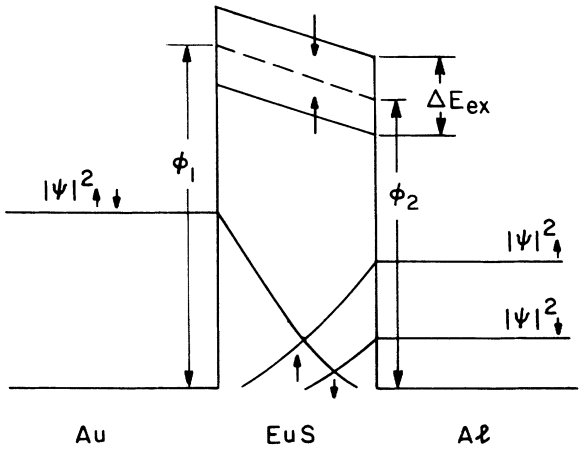

FIG. 1. The spin-filter model. The dashed line represents the tunnel barrier height at temperatures above T_m, and the solid lines the tunnel barrier heights for spin-up, -down electrons (as indicated by the arrows) for $T \ll T_m$. The tunneling probabilities for each spin-polarization are shown schematically as the overlap of the wave functions.

junction resistance below the ferromagnetic transition temperature of the barriers.[16,17]

We have reported the first direct observation of the spin-filter effect in a tunnel junction;[18] in this paper we present detailed studies of junctions with EuS barriers. There are three main experimental observations: (1) spin polarization of the tunnel current; (2) decrease of the junction resistance with temperature below 15 K; (3) the enhancement of the Zeeman splitting in the superconducting quasiparticle DOS in Al, and the initial Zeeman splitting in zero (applied) magnetic field as a special case. The first two observations are closely related and are both attributable to the spin-filter effect. The enhanced Zeeman splitting is a separate consequence of the ferromagnetic ordering in EuS; it is caused by the exchange interaction between the ordered magnetic Eu^{2+} ions and the conduction electrons in Al.

SAMPLE PREPARATION AND MEASUREMENTS

Junctions were made by evaporation of the materials onto glass substrates (Corning 7059). The thin Al electrode, 4.2 nm, was always deposited onto liquid-nitrogen-cooled substrates. The other metal electrode of Au, Ag, or Al (11 to 50 nm thick) and the barrier EuS were deposited onto either room-temperature substrates or liquid-nitrogen-cooled substrates. EuS was deposited through a rotating chopper which resulted in three different barrier thicknesses in one deposition, with a thickness ratio of 1:2:3. Typical values of nominal barrier thickness were 1.7, 3.3, and 5.0 nm. We found that EuS barriers of an approximate nominal thickness of 3 nm gave the best results. Tunneling conductance curves were taken in a ^{3}He cryostat at temperatures near 0.5 K. Magnetic fields parallel to the junction surface were provided by a superconducting solenoid. Tunnel junction resistance as a function of temperature was measured for some of the junctions from about 40 to 2 K.

SUPERCONDUCTOR-NORMAL METAL TUNNELING

The first direct observation of the spin-filter effect in a tunnel junction with a ferromagnetic barrier was obtained on Au/EuS/Al junctions, where the materials are listed in the sequence of their deposition. Figure 2 shows the tunnel conductance curves in various applied fields for one of the junctions with a Au counterelectrode. In this sample, the Au film is 11 nm thick, and the EuS film is 3.3 nm thick; both are deposited on room-temperature substrates. The 4.2-nm Al is deposited after the substrate is cooled to liquid-nitrogen temperature. The conductance curves in magnetic fields are highly asymmetrical with respect to zero voltage, indicating a strong spin polarization in the tunnel current.

We fitted the normalized dynamic conductance curves to the theory of thin-film superconductors in high mag-

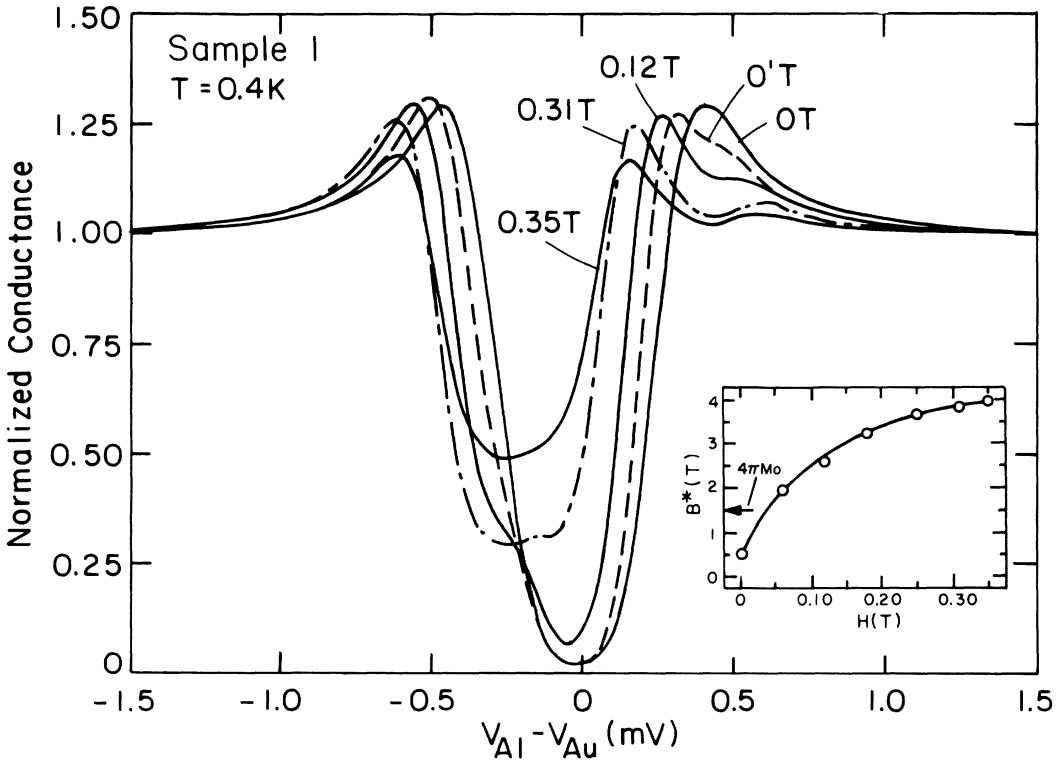

FIG. 2. Normalized dynamic conductance $(dI/DV_{SN})/(dI/DV_{NN})$ in various applied magnetic fields for Au/EuS/Al junction 1. The curve taken in zero field shows a small internal field which can be determined by fitting the curve to theory; B_i^* is found to be 0.5 T. Remanent Zeeman splitting corresponding to an internal field of about 2.0 T is seen in this junction. The inset shows the dependence of the internal field on the applied field. The saturation magnetization of EuS, $4\pi M_0 = 1.5$ T, is indicated by an arrow.

netic fields.[19] First, the densities of states for the two spin directions were calculated using the theory and convolved with the Fermi function (to obtain thermal broadening). The total conductance curve is a weighted sum of the two spin contributions:

$$dI/dV=\alpha(dI/dV)_{\uparrow}+(1-\alpha)(dI/dV)_{\downarrow}\ , \qquad (1)$$

where α is the number of spin-up electrons divided by the total number of electrons and polarization P is given by $2\alpha-1$. This total conductance was compared with the measured curve. Then, if necessary, the parameters were adjusted to generate another theoretical curve to be compared with the experimental one until they match. From the fits we found the polarization was 80% for junction 1.

The amount of Zeeman splitting in Al quasiparticle DOS was much bigger than the amount expected from the applied field. For example, junction 1 showed a Zeeman splitting which corresponded to a total effective field of 4.3 T in an applied field of only 0.35 T, indicating that the internal field B^* was close to 4 T. The field dependence of B^* on H is shown as the inset of Fig. 2. In all the junctions studied, a remanent Zeeman splitting persisted after the applied field was reduced to zero. Junction 1 showed a remanent Zeeman splitting corresponding to an internal field of 2 T.

Junction 1 also showed Zeeman splitting in the Al quasiparticle density of states before any magnetic field (except the ambient field of about 1 Oe) was applied. The initial Zeeman splitting is rather small in this junction; from fitting the curve the splitting was found to correspond to a field of $B_i^*=0.5$ T. We use B_i^* to indicate the effective field which corresponds to the *initial* zero-field Zeeman splitting (to be distinguished from the remnant zero-field splitting). One of the highest zero-field Zeeman splitting was observed in a Ag/EuS/Al junction (2) which showed an internal field $B_i^*\approx 3$ T. This junction also had a very high polarization of 85%. The value of B_i^* in the Ag/EuS/Al junction was so high that upon applying a field of less than 0.02 T the Al electrode reached its paramagnetic critical field B_{cp},[20] and became normal, so that only zero-field conductance was measured. It was difficult to determine the saturation value of B^* because the Al electrode became normal at very low applied fields (about 0.5 T), but $B^*_{\rm sat}$ was definitely much larger than the saturation magnetization of EuS, $4\pi M_0$, which is about 1.5 T.[12] (See the inset of Fig. 2.) This observation demonstrates that the extra Zeeman splitting cannot be explained as an effect of the EuS fringing field.

Junctions with the reversed sequence of deposition, that is, Al/EuS/Au, were also made. Here Al was deposited first onto a liquid-nitrogen cooled substrate, then the substrate was warmed up to room temperature and EuS and Au were deposited. The enhancement of the Zeeman splitting greatly diminished or even disappeared. The lack of an internal field was shown by both the tunneling data and the Al critical field data. The critical field of the Al film in these junctions was about 5 T which is the expected value for Al films about 4 nm thick,[1] and the Zeeman splitting of the Al quasiparticle DOS corresponded only to the external applied field.

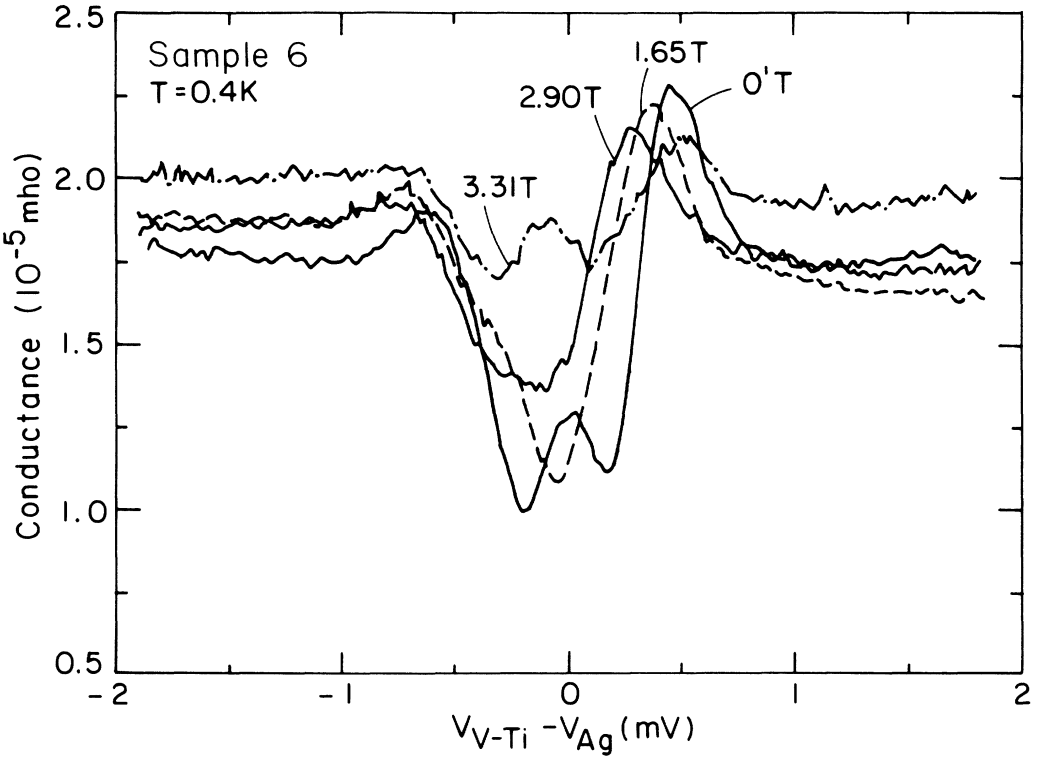

FIG. 3. Tunnel conductance curves in various applied magnetic fields for a Ag/EuS/V-Ti junction (6). There is spin polarization of the tunnel current and remanent zero-field Zeeman splitting. The curve labeled 0′ was taken after the applied field had been reduced to zero.

The disappearance of the enhanced Zeeman splitting was probably caused by a very thin layer of Al_2O_3 between the Al and the EuS films, which grew during the warming up (about an hour) of the substrates in a vacuum of 2×10^{-7} mm Hg and which destroyed the exchange interaction between the quasiparticles in Al and the magnetic Eu^{2+} ions. This observation is part of the experimental evidence that the cause of the extra Zeeman splitting is the exchange interaction at the EuS and Al interface, not the fringing field of the magnetization of EuS. The same conclusion was reached by Tkaczyk *et al.* in their study of the proximity effect of rare-earth-oxide/Al bilayers.[21]

Attempts at using other superconductors, such as V or a V-Ti alloy, as the spin-selective electrode were also made. Junctions of the type Ag/EuS/V/Al and Ag/EuS/VTi/Al were fabricated, in which the top 1.5-nm Al film was used as a protective layer for the 10-nm V or V-Ti thin films. One Ag/EuS/VTi junction (6) with 10-nm EuS showed spin polarization of the tunnel current as seen from the asymmetry of the tunnel conductance curves (see Fig. 3). However, the junction had too high a leakage current which made quantitative analysis of the data difficult. Often junctions with a V or a V-Ti electrode were depaired at zero field with considerable leakage current.

SUPERCONDUCTOR-SUPERCONDUCTOR TUNNELING

Electron spin polarization in the tunnel current was observed in superconductor-superconductor (*S-I-S*) tunnel junctions as well. Two Al/EuS/Al junctions (4 and 5) from the same evaporation were studied extensively. All the junctions consisted of bottom Al electrodes (50 nm thick), the EuS barrier with nominal thickness 3.3 nm, and a top Al film of 4.2 nm. They all showed Zeeman splitting in zero applied magnetic field. Since no Zeeman splitting is observable in *S-I-S* tunneling if the densities of states of both of the superconducting electrodes are split by the same amount,[22] we assume that the bottom electrode is not much affected by the EuS. Two factors support this assumption: (1) the possible growth of some oxide on the Al bottom electrode before the deposition of the EuS barrier would weaken the average exchange interaction, and (2) the inverse proportion of the average exchange field to the superconductor film thickness[23] further reduces the proximity effect on the thicker Al electrode.

The *S-I-S* tunneling conductance curves are shown in Fig. 4. Both curves were taken without any applied magnetic field. There is clearly initial zero-field Zeeman splitting; from fitting the curves we found that $B_i^*=1.9$ T in junction 4 and $B_i^*=2.6$ T in junction 5. The peaks in the conductance curves were identified with the help of the schematic drawing in Fig. 5, which depicts the situation in which one of the superconducting electrodes is subjected to a magnetic field B^*, and the other is not affected. For simplicity we have left out the spin-filter effect in Fig. 5.

If B^* were equal to zero (not shown in Fig. 5), there would be two sum peaks at $\Delta_1+\Delta_2$ and $-(\Delta_1+\Delta_2)$ and two difference peaks at $\Delta_1-\Delta_2$ and $-(\Delta_1-\Delta_2)$, where Δ_1 and Δ_2 are the superconducting half-gaps of the top and bottom electrodes, respectively. However, as shown in Fig. 5, when $B^*\neq0$, for $\mu B^*>|\Delta_1-\Delta_2|$ (where μ is the Bohr magneton), there will be six peaks in the conductance curve. On the positive-bias side ($V_{top}-V_{bottom}>0$), there are the spin-down difference peak at $\mu B^*-(\Delta_1-\Delta_2)$ and two sum peaks, spin-up at $\Delta_1+\Delta_2-\mu B^*$ and spin-down at $\Delta_1+\Delta_2+\mu B^*$; on the negative-bias side, there are the spin-up difference peak at $-\mu B^*+(\Delta_1-\Delta_2)$ and two sum peaks, spin-down at $-\Delta_1-\Delta_2+\mu B^*$ and spin-up at $-(\Delta_1+\Delta_2+\mu B^*)$. If $\mu B^*<|\Delta_1-\Delta_2|$, there will still be six peaks in the conductance curve, but the two difference peaks are reversed in their spin directions. The conductance curves in Fig. 4 are asymmetrical because the spin-filter effect of the EuS makes all the spin-up peaks larger than their spin-down counterparts.

Fitting the dynamic conductance curves of *S-I-S* tunneling is similar to fitting those of *S-I-N* tunneling. The DOS for both electrodes have to be calculated using the

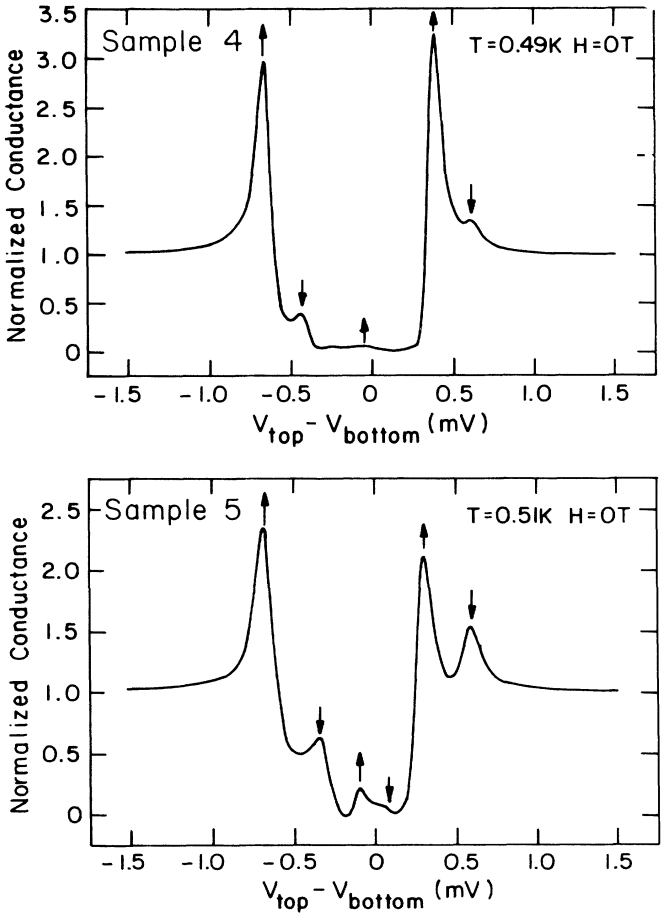

FIG. 4. Normalized *S-I-S* tunnel conductance curves for two Al/EuS/Al junctions made in the same evaporation, in zero applied magnetic field. The spin directions of the peaks are labeled by the up or down arrows. $B_i^*=1.9$ T and $P=85\%$ for Sample 4, and $B_i^*=2.6$ T and $P=60\%$ for Sample 5.

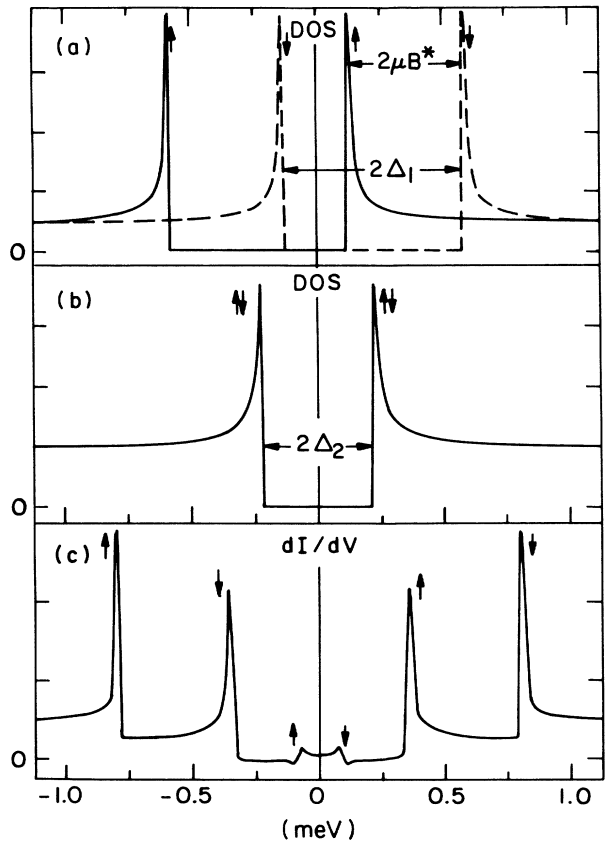

FIG. 5. Schematic of a superconductor-superconductor tunnel conductance curve where the DOS of only one of the electrodes (top) is Zeeman split by a field B^*. (a) and (b) show the densities of states of the top and bottom electrodes, respectively, and (c) is a computer-simulated tunnel conductance curve between the two superconductors in (a) and (b). The peaks in the total conductance curve are labeled by the up or down arrows which indicate the corresponding spin directions.

theory of Ref. 19, but instead of convolving one DOS with a constant (the density of states of normal metals at the Fermi level) and the Fermi function, the convolution is carried out over the two superconducting densities of states and the Fermi function. The total conductance is the same weighted sum as in Eq. (1). From the fits the value of polarization in junction 4 is found to be about 85% and in junction 5 about 60%. These junctions were made in the same deposition and had the same nominal EuS barrier thickness. Why their values of polarization differ by a large amount is not clear to us at the moment. Local variations of the effective barrier thickness can explain some of the difference but not all.

JUNCTION RESISTANCE AS A FUNCTION OF TEMPERATURE

The decrease of junction resistance with temperature below the ferromagnetic transition temperature of EuS is another manifestation of the spin-filter effect. We have measured the tunnel current I as a function of the applied voltage V for one junction, and R_J versus T for most of the junctions studied, from about 40 to 2 K. All of the measurements were made in zero magnetic field.

Some I-V characteristics from 3 (which is an Al/EuS/Al junction similar to 4 and 5) and their fits to Simmon's theory[24] are shown in Fig. 6. For a trapezoidal barrier, the tunnel current density, for each spin direction, is given by

$$J_{\uparrow,\downarrow}=J_0\left[\phi_{\uparrow,\downarrow}-\frac{eV}{2}\right]\exp\left[-A\left[\phi_{\uparrow,\downarrow}-\frac{eV}{2}\right]^{1/2}\right] -J_0\left[\phi_{\uparrow,\downarrow}+\frac{eV}{2}\right]\exp\left[-A\left[\phi_{\uparrow,\downarrow}+\frac{eV}{2}\right]^{1/2}\right], \tag{2}$$

where $J_0=(e/2\pi h)S^{-2}$, $A=(4\pi S/h)(2m_e)^{1/2}$ with m_e being the electron mass. We used the following method to fit the I-V curves. First, I-V curves taken at 31, 21, and 18 K were fitted to obtain values of the barrier thickness S and the barrier height ϕ_0, which were, respectively, 16.4 Å and 2.08 eV. Then, I-V curves taken at temperatures from 1.3 to 15 K were fitted using EuS conduction-band splitting ΔE_{ex} as the fitting parameter and keeping S and ϕ_0 constant at the values obtained from the first step. From these fits, ΔE_{ex} as a function of temperature was obtained. The maximum barrier lowering (which is assumed to be one-half of the maximum EuS conduction-band splitting) in our case was 0.28 eV, considerably larger than the optical measurement of 0.18 eV.[13]

Figure 7 shows R_J versus T data. The junction resistances were essentially constant from 77 to 30 K (not shown); the decrease of R_J started at about 15 K. Using optically measured $\Delta E_{ex}(T)$ (Ref. 13) and Eq. (1) we calculated S and ϕ_0 (see the last two columns of Table I) from the measured $R_J(2\text{ K})/R_J(35\text{ K})$ and $R_J(2\text{ K})$ and obtained the value of polarization, $P=(J_\uparrow-J_\downarrow)/(J_\uparrow+J_\downarrow)$. Table I compares the calculated and measured values of polarization. The value of polarization inferred from the resistance ratio is in general larger than the one measured from the tunnel conductance asymmetry. Moreover, one particular junction resistance ratio is always associated with a certain polarization. For example, for junction 3, using S, ϕ_0, and $\Delta E_{ex}(2\text{ K})$ obtained from fitting the I-V curves, we got the same $R_J(2\text{ K})/R_J(35\text{ K})=0.38$ and $P=91.6\%$.

The maximum EuS conduction-band splitting we obtained from fitting the I-V curves is much larger than the optical measurement on single crystals. This is implausible, especially since T_m of our EuS films has not increased from the bulk value. This and the high polarization values implied by the junction resistance change suggest that there may be additional factors besides the EuS conduction-band splitting that are responsible for the junction resistance decrease. Thompson *et al.*[17] observed a sixfold decrease in the resistance in a Schottky tunnel barrier between a In metal and Gd-doped EuS. They attributed this decrease in resistance to the suppression of magnetic scattering in the tunnel barrier at temperatures

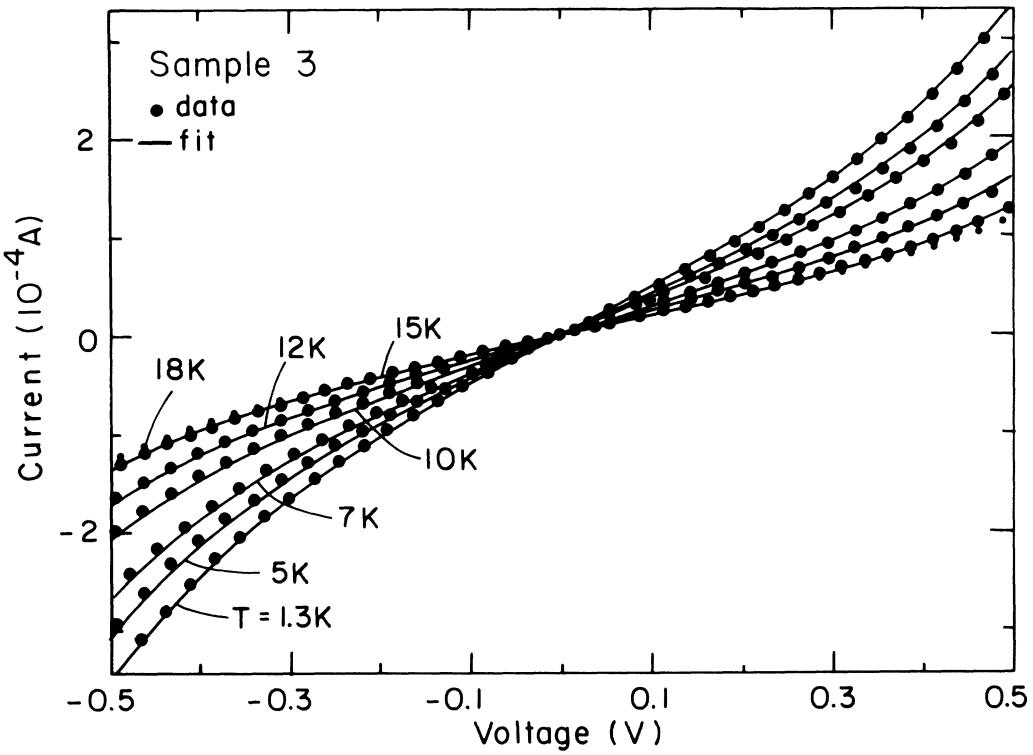

FIG. 6. *I-V* characteristics of junction 3 at various temperatures. The dots represent the data; the solid lines are fits to Eq. (2). Above 15 K, the *I-V* curves basically fall on top of each other. The smaller dots (which almost coincide with the 15 K data) are *I-V* at $T=18$ K; *I-V* curves at higher temperatures are not shown for clarity.

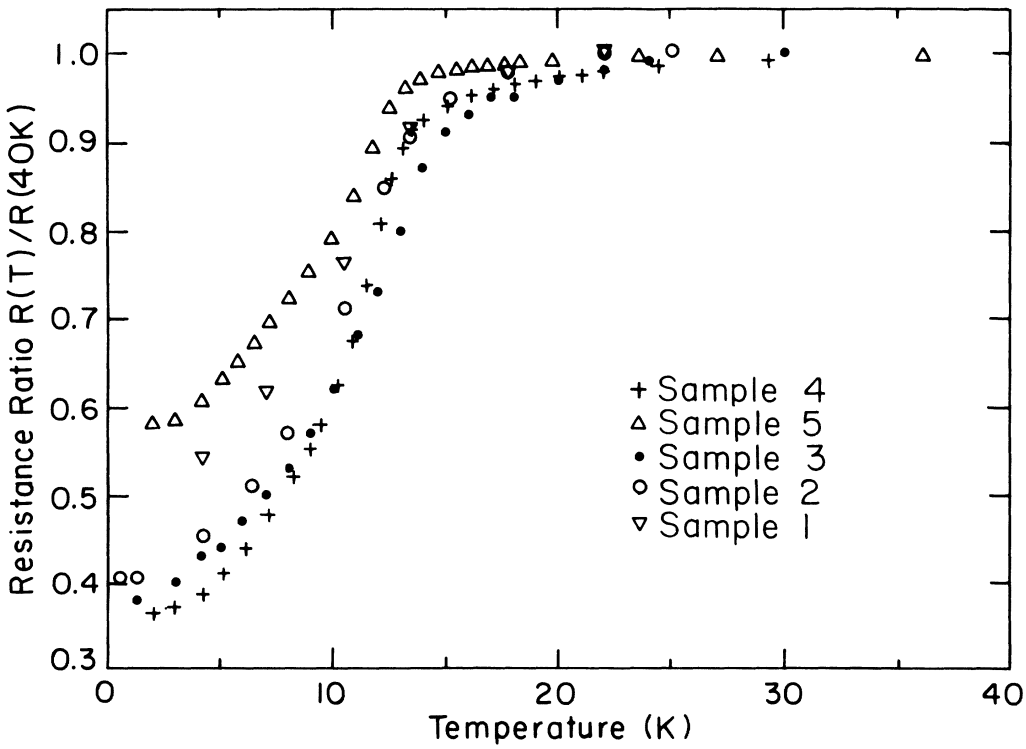

FIG. 7. Junction resistance as a function of temperature. The sharp decrease of R_J indicates the onset of the ferromagnetic transition in the EuS barrier, which is approximately between 14 to 15 K for these films.

TABLE I. Comparison of values of polarization. P_{meas} is the value measured from the tunnel conductance curve asymmetry. P_{calc} is calculated using Eq. (2) and the optically measured $\Delta E_{ex}(T)$.

Junction	Sample no.	P_{meas} (%)	P_{calc} (%)	$\frac{R_J(2\text{ K})}{R_J(35\text{ K})}$	$R_J(2\text{ K})$ (kΩ)	S (Å)	ϕ_0 (eV)
Au/EuS/Al	1	80	84.9	0.51	0.3	17.8	1.56
Ag/EuS/Al	2	85	90.8	0.40	0.47	19.8	1.32
Al/EuS/Al	3	85	91.6	0.38	2.2	20.4	1.32
Al/EuS/Al	4	85	92.6	0.36	14.4	21.9	1.42
Al/EuS/Al	5	60	80.4	0.58	3.0	17.6	1.96

below T_m. Their experiment with degenerate semiconducting EuS cannot be directly compared with our experiment; however, we did try to measure $R_J(T)$ in various applied fields. We found that there was no evidence of the kind of magnetic scattering reported by Thompson *et al.* in our junctions. The discrepancy between the measured and the calculated values of P remains unexplained.

DISCUSSION

As mentioned earlier, some junctions showed Zeeman splitting in the conductance curve before any external magnetic field was applied; the initial Zeeman splitting was sample dependent. Whether the initial zero-field Zeeman splitting can be observed or not depends on the size of magnetic domains in EuS. In junctions where EuS was deposited onto liquid-nitrogen-cooled substrates, the crystallites are small and the domain sizes are likely to be small so that we seldom observed initial zero-field Zeeman splitting. When $L \ll \xi$, where L is the representative domain size and ξ the superconducting coherence length, the exchange field averaged over an area ξ^2 is zero. When an external field is applied, the domains which have a magnetization direction parallel to the applied field will grow giving rise to an average exchange field which increases with the applied field. The inset of Fig. 2 shows the internal field B^* as a function of the applied field for junction 1. If $L \geq \xi$, then the average exchange field may be nonzero even without any applied field.

In contrast to the field dependence of B^*, the value of polarization does not change with the applied field. To understand this we must first understand how spin polarization is determined in tunneling experiments. It is calculated from the asymmetry of the conductance curve.[7] The splitting of the EuS conduction band in each domain

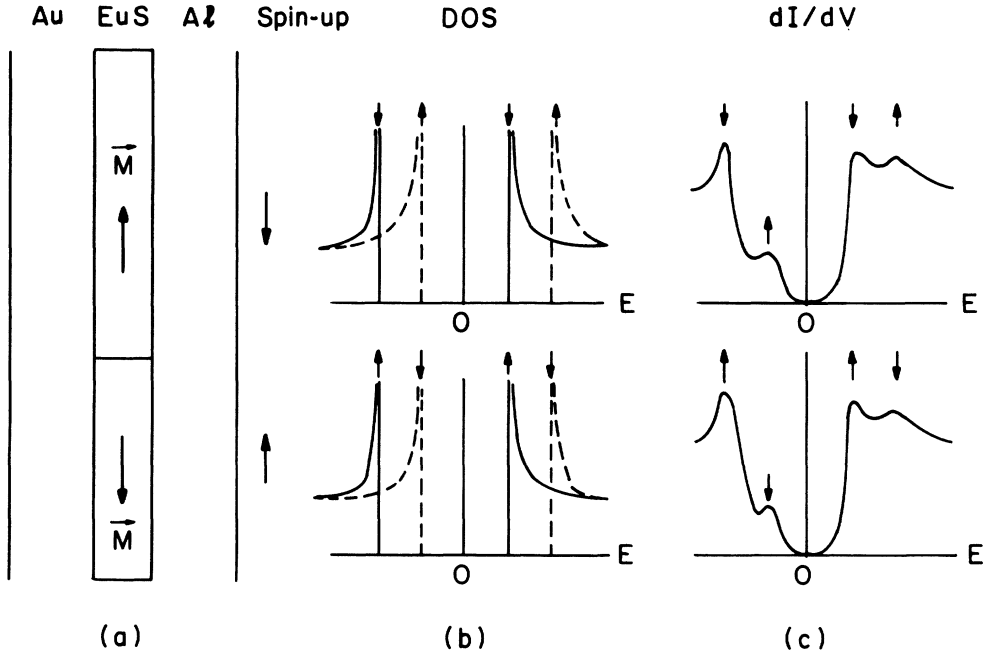

FIG. 8. Contributions to the tunnel conductance from two opposite domains in the EuS barrier. (a) shows schematically the cross section of a tunnel junction with an area on the order of ξ^2. (b) The amount of Zeeman splitting in the Al quasiparticle DOS is determined by the area-averaged magnetization. (c) Each domain favors the tunneling of electrons which have spin-up polarization as defined by the magnetization of that domain, but the overall tunnel conductance has the same functional form regardless of the domain orientation.

favors the tunneling of electrons whose spin direction is antiparallel (spin up) to the magnetization direction of that domain; therefore, each domain contributes to the conductance asymmetry in the same manner. Figure 8 illustrates this graphically. Suppose the two magnetic domains in Fig. 8 span an area on the order of ξ^2. Then the DOS of Al is split by an effective field that is related to the area-averaged magnetization. Electrons which tunnel through either of the two domains see the same Zeeman splitting in the quasiparticle DOS. However, the labeling of the spin polarization of the DOS branches is relative to the magnetization direction of the domain through which the electrons tunnel. The spin-filter effect favors the tunneling of electrons with spin-up polarization which is antiparallel to the magnetization direction of the domain. Since these are the electrons of lowest energy, the conductance curve as a function of energy will have the same shape for each domain, independent of its absolute direction of magnetization. Therefore, changing the domain sizes will change the amount of Zeeman splitting, but not the polarization. Since the domains of the EuS in zero field will be so arranged such that there is little overall magnetization, one could say that compared with some external direction the spin polarization of the tunneling electrons is near zero. Only when the junction area, which is about 3×10^{-3} cm^2, consists of one single domain (in zero field) is the tunnel current truly polarized with respect to a external reference direction; of course, this can be achieved by aligning the domains using external fields. It would be helpful to know the domain sizes in zero applied field in the EuS barrier.

In studying the proximity effect in tunnel junctions of the type *R*- (or *RO*-) Al/Al_2O_3/Fe (*R* stands for rare-earth metals and *RO* rare-earth oxides), Tkaczyk *et al.* identified the exchange interaction between the quasiparticles in Al and the magnetic Eu^{2+} ions in EuS as the cause of the enhanced Zeeman splitting in the Al density of states.[21] In their study, they did not observe any appreciable reduction of the superconducting transition temperature in the EuO/Al bilayer as compared with pure Al. If the exchange interaction were the cause of the effective internal field B^*, then there should be depairing according to the theory of Abrikosov and Gor'kov (AG).[25] Tkaczyk and co-workers gave the following explanation. The average effective field B^* caused by exchange interaction is a first-order effect, $B^*\sim cJ\langle S_i\rangle$ (where c is the concentration of the magnetic impurity, J the exchange constant, S_i the total angular momentum of the magnetic impurity, and $\langle S_i\rangle$ represents the thermal average); depairing is a second-order effect, $\Delta T_c\sim cJS_i(JS_i/E_F)$ (E_F is the Fermi energy of Al). While B^* was observable, the reduction of T_c was too small (≤0.05 K) to be seen owing to the small exchange constant. They estimated J to be 3.5 meV for oxidized Eu.

We also measured the superconducting transition temperatures of Al in the EuS/Al bilayer as compared with that of a control Al strip made in the same evaporation. Sometimes there was a T_c reduction in EuS/Al, sometimes there was not. Furthermore, we have noticed that a reduction of T_c was always accompanied by the existence of the initial zero-field Zeeman splitting. This result is not in conflict with that of Tkaczyk *et al.* In their case, the oxidized Eu was not ordered in zero magnetic field; therefore, the depairing effect came from the paramagnetic impurities as described by the AG theory. Frequently, in our case, the EuS *was* ordered in zero field, so besides the AG impurity depairing, there was extra depairing coming from the exchange field B_i^*, which acts only on the quasiparticle spins. The problem of a magnetic field interacting only with the superconducting conduction electron spins and not on the orbits has been formulated by several theorists;[26,27] the bilayer of EuS/Al provides an experimental system for such a study, and its investigation is being carried out.

Conservation of electron spins in the tunneling process has been shown to hold to high accuracy in Al/Al_2O_3/Al junctions[22] and was assumed in and is consistent with the present analysis. After the conduction band in EuS splits into spin-polarized subbands, electrons with up spins tunnel through the spin-up conduction subband, and electrons with down spins tunnel through the spin-down subband. This is the basis for the existence of the spin-filter effect.

CONCLUSION

In summary, we have observed directly, in a tunnel junction, the spin-filter effect of the ferromagnetic EuS barrier. The spin polarization of the tunnel electrons is as high as 85%. The spin-filter effect is also manifested by the decrease of the junction resistance below 15 K. Moreover, the magnetic ordering in EuS gives rise to a large exchange field which acts on the spins of the electrons in Al, causing zero-field Zeeman splitting in the superconducting quasiparticle DOS. The spin-filter effect may be used to provide a low-energy spin-polarized electron source and the zero-field Zeeman splitting in the DOS makes it possible to have a spin-selective tunnel electrode without any external magnetic field. Both may be useful in applications.

ACKNOWLEDGMENTS

We thank Richard MacNabb for fabricating the junctions and P. M. Tedrow for providing useful information. One of the authors (X.H.) also wishes to thank M. S. Dresselhaus for stimulating discussions at various stages of the work. This work is supported by the National Science Foundation under Grant Nos. DMR-8619087 and DMR-8822744.

[1]R. Meservey, P. M. Tedrow, and P. Fulde, Phys. Rev. Lett. **25**, 1270 (1970).
[2]P. M. Tedrow and R. Meservey, Phys. Lett. **69A**, 285 (1978).
[3]G. A. Gibson and R. Meservey, Phys. Rev. B **40**, 8705 (1989).
[4]P. M. Tedrow and R. Meservey, Phys. Lett. **51A**, 57 (1975).
[5]G. A. Gibson, P. M. Tedrow, and R. Meservey, Phys. Rev. B **40**, 137 (1989).
[6]S. J. Bending, M. R. Beasley, and C. C. Tsuei, Phys. Rev. B **30**, 6342 (1984).
[7]P. M. Tedrow and R. Meservey, Phys. Rev. B **7**, 318 (1973).
[8]D. Paraskevopoulos, R. Meservey, and P. M. Tedrow, Phys. Rev. B **16**, 4907 (1977).
[9]R. Meservey, D. Paraskevopoulos, and P. M. Tedrow, Phys. Rev. B **22**, 1331 (1980).
[10]R. Meservey, P. M. Tedrow, and J. S. Moodera, J. Magn. Magn. Mater. **35**, 1 (1983).
[11]M. B. Stearns, J. Magn. Magn. Mater. **5**, 167 (1977).
[12]For review of properties of the Eu chalcogenides, see P. Wachter, in *Handbook on the Physics and Chemistry of Rare Earths,* edited by K. A. Gschneidner, Jr. and L. Eyring (North-Holland, Amsterdam, 1979), Chap. 19; also see the next reference, Ref. 13.
[13]P. Wachter, CRC Crit. Rev. Solid State Sci. **3**, 189 (1972).
[14]N. Müller, W. Echstein, W. Heiland, and W. Zinn, Phys. Rev. Lett. **29**, 1651 (1972).
[15]E. Kisker, G. Baum, A. H. Mahan, W. Raith, and K. Schröder, Phys. Rev. Lett. **36**, 982 (1976); E. Kisker, G. Baum, A. H. Mahan, W. Raith, and B. Reihl, Phys. Rev. B **18**, 2256 (1978).
[16]L. Esaki, P. J. Stiles, and S. von Molnar, Phys. Rev. Lett. **19**, 852 (1967).
[17]W. A. Thompson, F. Holtzberg, T. R. McGuire, and G. Petrich, in *Magnetism and Magnetic Materials (Chicago, 1971),* Proceedings of the 17th Annual Conference on Magnetism and Magnetic Materials, AIP Conf. Proc. No. 5, edited by C. D. Graham, Jr. and J. J. Rhyne (AIP, New York, 1972), p. 827.
[18]J. S. Moodera, X. Hao, G. A. Gibson, and R. Meservey, Phys. Rev. Lett. **61**, 637 (1988).
[19]J. A. X. Alexander, T. P. Orlando, D. Rainer, and P. M. Tedrow, Phys. Rev. B **31**, 5811 (1985).
[20]A. M. Clogston, Phys. Rev. Lett. **9**, 266 (1962).
[21]J. E. Tkaczyk, Ph.D. thesis, Massachusetts Institute of Technology, 1988 (unpublished); J. E. Tkaczyk and P. M. Tedrow, J. Appl. Phys. **61**, 3368 (1987); P. M. Tedrow, J. E. Tkaczyk, and A. Kumar, Phys. Rev. Lett. **56**, 1746 (1986).
[22]P. M. Tedrow and R. Meservey, Phys. Rev. Lett. **27**, 919 (1971).
[23]P. G. de Gennes, Phys. Lett. **23**, 10 (1966).
[24]J. G. Simmons, J. Appl. Phys. **34**, 1793 (1963).
[25]A. A. Abrikosov and L. P. Gor'kov, Zh. Eksp. Teor. Fiz. **39**, 1781 (1960) [Sov. Phys.—JETP **12**, 1243 (1961)].
[26]G. Sarma, J. Phys. Chem. Solids **24**, 1029 (1963).
[27]P. Fulde and K. Maki, Phys. Rev. **141**, 275 (1966); **147**, 414(E) (1966). Also see the review article by P. Fulde, Adv. Phys. **22**, 667 (1973).